

## $\beta$ decay of the $\pi f_{5/2}$ ground state of $^{77}\text{Cu}$ studied with 225 MeV and 0.2 MeV purified radioactive beams

S. V. Ilyushkin,<sup>1,\*</sup> J. A. Winger,<sup>1</sup> C. J. Gross,<sup>2</sup> K. P. Rykaczewski,<sup>2</sup> J. C. Batchelder,<sup>3</sup> L. Cartegni,<sup>4</sup> I. G. Darby,<sup>4,5</sup> C. Goodin,<sup>6</sup> R. Grzywacz,<sup>2,4</sup> J. H. Hamilton,<sup>6</sup> A. Korgul,<sup>4,6,7,8</sup> W. Królas,<sup>8,9</sup> S. N. Liddick,<sup>3,4</sup> C. Mazzocchi,<sup>4,10</sup> S. Padgett,<sup>4</sup> A. Piechaczek,<sup>11</sup> M. M. Rajabali,<sup>4</sup> D. Shapira,<sup>2</sup> and E. F. Zganjar<sup>11</sup>

<sup>1</sup>*Department of Physics and Astronomy, Mississippi State University, Mississippi State, Mississippi 39762, USA*

<sup>2</sup>*Physics Division, Oak Ridge National Laboratory, Oak Ridge, Tennessee 37831, USA*

<sup>3</sup>*UNIRIB, Oak Ridge Associated Universities, Oak Ridge, Tennessee 37831, USA*

<sup>4</sup>*Department of Physics and Astronomy, University of Tennessee, Knoxville, Tennessee 37996, USA*

<sup>5</sup>*Instituut voor Kern-en Stralingsfysica, Katholieke Universiteit Leuven, Leuven B-3001, Belgium*

<sup>6</sup>*Department of Physics and Astronomy, Vanderbilt University, Nashville, Tennessee 37235, USA*

<sup>7</sup>*Institute of Experimental Physics, Warsaw University, Warszawa PL-00-681, Poland*

<sup>8</sup>*Joint Institute for Heavy-Ion Reactions, Oak Ridge, Tennessee 37831, USA*

<sup>9</sup>*Institute of Nuclear Physics, Polish Academy of Sciences, Kraków PL-31-342, Poland*

<sup>10</sup>*Università degli Studi di Milano and INFN, Sez. Milano, Milano I-20133, Italy*

<sup>11</sup>*Department of Physics and Astronomy, Louisiana State University, Baton Rouge, Louisiana 70803, USA*

(Received 12 August 2009; published 6 November 2009)

Isobarically purified beams of  $^{77}\text{Cu}$  with energies of 225 and 0.2 MeV were used at the Holifield Radioactive Ion Beam Facility of Oak Ridge National Laboratory to study  $\beta$  decay into states in  $^{77}\text{Zn}$ . Data taken at 225 MeV allowed the determination of absolute branching ratios relative to the decay of  $^{77}\text{Cu}$  for this  $\beta$  decay as well as its daughters. From these we obtained a refined  $\beta$ -delayed neutron emission probability of 30.3(22)% and a probability that the decay proceeds through  $^{77}\text{Zn}^g$  of 49.1(26)%. A total of 64  $\gamma$  rays were placed in a level scheme for  $^{77}\text{Zn}$  containing 35 excited states including one state above the neutron separation energy, whereas two  $\gamma$  rays were observed for the  $\beta n$  branch to states in  $^{76}\text{Zn}$ . The growth and decay curves of some prominent  $\gamma$  rays indicate a single  $\beta$ -decaying state with a half-life of 480(9) ms. The decay pattern for  $^{77}\text{Cu}$ , with observed feeding of 8(3)% to  $7/2^+$   $^{77}\text{Zn}^g$  and 6(3)% to  $1/2^-$   $^{77}\text{Zn}^m$ , in contrast to the large feeding observed for decay of  $\pi p_{3/2}$   $^{73}\text{Cu}^g$  to  $1/2^-$   $^{73}\text{Zn}^g$ , strongly suggests a  $\pi f_{5/2}$  ground state for the studied  $^{77}\text{Cu}$  activity.

DOI: [10.1103/PhysRevC.80.054304](https://doi.org/10.1103/PhysRevC.80.054304)

PACS number(s): 23.20.Lv, 23.35.+g, 27.50.+e, 29.38.-c

### I. INTRODUCTION

The study of nuclei far from stability has led to many surprises, as our understanding of nuclei near stability does not project well to extremely proton-rich or neutron-rich regions. The disappearance and reappearance of shells suggest a very dynamic aspect to the nuclear force that must be understood as we proceed even farther from stability. The migration of neutron or proton orbitals will affect the  $\beta$ -decay strength function above the neutron or proton separation energy, creating changes in the conditions for  $\beta$ -delayed nucleon emission. Therefore, an understanding of the processes behind single-particle energy (SPE) variations is important in evaluating the decay behavior of neutron- or proton-rich nuclei.

Many of our assumptions about the locations of shell closures must be modified as we move away from stability because the magic numbers extracted from nuclei near stability and that appear to be valid for some regions far from stability fail to hold up in others [1,2]. This appears to be especially true for the  $28 < N \leq 50$  region for neutron-rich nuclei as  $^{78}\text{Ni}$  is approached. Results of previous studies [3] have shown lowering of the  $\pi f_{5/2}$  orbit relative to the  $\pi p_{3/2}$  orbit as the  $\nu g_{9/2}$  orbital is being filled. These orbital

variations have been shown to be due to an attractive monopole interaction between neutrons occupying the  $\nu g_{9/2}$  state and protons in the  $\pi p_{3/2}$  orbital [4]. In addition, a consistent description of weakly bound systems requires attention to the effects of open channels and many-body correlations [5]. The result is the disappearance of old shells and the appearance of new shells that can significantly affect the low-energy structure and  $\beta$ -delayed neutron emission probabilities for nuclei in this region [6].

Because there is significant theoretical and experimental evidence that the  $\pi p_{3/2}$  and  $\pi f_{5/2}$  states will cross for neutron-rich Cu isotopes [3,4], determination of when this crossing occurs and the rate at which the SPE changes as a function of neutron number is very important. In this article we present evidence that the ground state in  $^{77}\text{Cu}$  must be the  $\pi f_{5/2}$  state.

### II. EXPERIMENTAL TECHNIQUE

The experiment was performed using the Holifield Radioactive Ion Beam Facility at Oak Ridge National Laboratory. Beams of Cu ions were produced by proton-induced fission of a  $\text{UC}_x$  target. Results of two separate experiments are reported here. In the first experiment, Cu ions were accelerated to 225 MeV by the Oak Ridge National Laboratory tandem

\* [svil@msstate.edu](mailto:svil@msstate.edu)

accelerator before being sent to a detector station using the so-called “ranging-out” (RO) mode [7]. Results on  $\beta$ -delayed neutron emission probabilities based on this experiment were reported previously [6]. In the second experiment, low-energy ions (200 keV) were sent directly to the newly commissioned Low-energy Radioactive Ion Beam Spectroscopy Station (LeRIBSS) for study [8]. The LeRIBSS benefits from its location just past the high-resolution injector magnet and before the tandem accelerator, where the highest quality and intensity beams are available. The fact that acceleration is not required permits experiments with negative as well as positive ions, and skipping of the tandem accelerator gives a factor of 10 gain in beam intensity. In both cases, the ions passed through a charge exchange cell that removed all zinc ions from the beam. This, along with careful tuning of the high-resolution isobar separator and/or selective RO, provided highly purified beams of Cu ions for these studies. In the RO experiment the beam purity was measured as  $\sim 68\%$ , with  $^{77}\text{Ga}$  being the only significant contaminant. In the LeRIBSS experiment, a comparison of  $\gamma$  rays from  $^{77}\text{Cu}$  and  $^{77}\text{Ga}$  decays indicated that a similar purity was obtained. For both measurements, the collected activity was observed by four clover Ge detectors and two plastic  $\beta$  detectors in air around the 0.5-mm thin-aluminum beam pipe. All signals were read out using digital electronics [9]. In the LeRIBSS configuration, the closely packed clover array had a measured peak efficiency of 29% at about 100 keV and an efficiency of 5% at 1.33 MeV. Additional information on the RO setup is given in Refs. [6,7,10–12]. The main features of the techniques used in the two experiments are presented in the following paragraphs.

In the first experiment, accelerated ions with an average rate of about 15 ions/s were time-tagged using a microchannel plate detector, passed through a six-segment ion chamber (IC), and implanted on the tape of a moving tape collector (MTC) with a tape transport time of 525 ms. Owing to passage through the IC, the ions could be clearly identified by energy loss in the six segments and counted on an event-by-event basis. This allowed for easy tuning of the high-resolution isobar separator to optimize the beam for rate and purity as well as to measure the absolute number of  $^{77}\text{Cu}$  ions in the studied samples. Using this setup allows for two modes of operation, the pass-through and RO modes, as described previously [6,7,10–12]. Presented herein are results based on data obtained in the pass-through mode, in which the IC was run at a low pressure, ensuring that more than 99% of the identified and counted  $^{77}\text{Cu}$  ions would exit the IC and be implanted on the MTC at a point in the center of the detector array. With the system running in this mode, an exact count of the number of ions implanted on the MTC could be made, allowing for the direct determination of absolute branching ratios. The MTC cycle used involved a period of beam deposition while the decays were observed, followed by movement of the tape to a shielded location to remove long-lived daughters before starting the next cycle. Because the Zn ions were removed from the beam, the MTC cycle time was set to limit the buildup of  $^{77}\text{Ga}$  [ $t_{1/2} = 13.2(2)$  s] in the sample. Data were collected using a 7-s MTC cycle. Additional data were obtained while the system was running with the beam in saturation. All  $\gamma$ -ray intensities for this

experiment were determined using the  $\gamma$ -ray singles spectra, which were used only to determine absolute branching ratios.

The LeRIBSS was used to perform a second study on  $^{77}\text{Cu}$   $\beta$  decay. Again, the charge exchange cell was used to remove  $^{77}\text{Zn}$  ions. Because the beam was not accelerated, there was an approximately one order-of-magnitude gain in beam intensity at an average rate of about 130 ions/s. Improvements in tuning of the high-resolution isobar separator allowed us to achieve a high-purity beam of  $^{77}\text{Cu}$  ions without using the RO technique. Additional improvements over the first experiment included the implementation of a system to rapidly deflect the beam before the high-resolution isobar separator, which allowed for study of the growth and decay of the deposited sources. In addition, the LeRIBSS utilizes a new MTC with a transport time of 210 ms, making it a better choice for the study of short-lived nuclei. A typical MTC cycle included a growth period with beam deposition, deflection of the beam for a decay period, and then movement of the tape, with data obtained during both the growth and the decay periods. A 3-s growth/3-s decay MTC cycle was used in the study of  $^{77}\text{Cu}$ . Finally, a saturation measurement was made. Because  $^{77}\text{Cu}$  was the primary component of the beam, none of the daughter activities became dominant in the spectrum. A representative  $\beta$ -gated spectrum from the saturation measurement is shown in Fig. 1. A portion of this spectrum taken in the  $\gamma$ -ray singles mode is shown in Fig. 2, which indicates the presence of the 772-keV  $\gamma$  ray depopulating the  $J^\pi = 1/2^-$   $^{77}\text{Zn}^m$ , as discussed in more detail later. Analysis of these spectra as well as  $\gamma$ - $\gamma$  coincidence data allowed construction of the decay scheme shown in Fig. 3.

Relative  $\gamma$ -ray intensities reported here were taken from the LeRIBSS measurement. For stronger  $\gamma$  rays it was possible to extract these intensities from the  $\gamma$ -ray singles spectrum. However, identifying weaker  $\gamma$  rays and determining their relative intensities required the use of a  $\beta$ -gated spectrum (Fig. 1). To extract the correct relative intensities for these  $\gamma$  rays, it was necessary to determine the  $\beta$  detection efficiency ( $\beta_{\text{eff}}$ ) for  $\gamma$  rays depopulating any given level. This efficiency was found to range from 15% to 65%, depending on the  $\beta$  energies of the levels fed, which in turn determine the fraction of the  $\beta$  particles that could reach the  $\beta$  detectors. For some levels there was a strong transition (e.g., 957 and 1926 keV), which allowed the direct determination of  $\beta_{\text{eff}}$ , whereas for a number of levels it was necessary to obtain a reasonable estimate of this value. Obtaining these estimates was based on some simple assumptions. First,  $\beta_{\text{eff}}$  should be a smoothly varying function of the maximum  $\beta$  energy directly feeding a level, as different fractions of the  $\beta$ -energy spectrum are being sampled. Second, over a range of a few mega-electron volts,  $\beta_{\text{eff}}$  will vary linearly. These assumptions allow us to define an effective  $Q$  value ( $Q_{\text{eff}}$ ) based on both direct and indirect feeding of the level as determined from the decay scheme. Doing this is problematic, as missing  $\gamma$  rays in the decay scheme will result in too high a value for  $Q_{\text{eff}}$ . The choice of  $\gamma$  rays used to establish the efficiency curve was therefore limited to those  $\gamma$  rays for which it was reasonable to assume that the feeding had been correctly determined. This uncertainty in the feeding results in cases in which  $\beta_{\text{eff}}$  is very precisely known but  $Q_{\text{eff}}$  has a large uncertainty. Conversely,

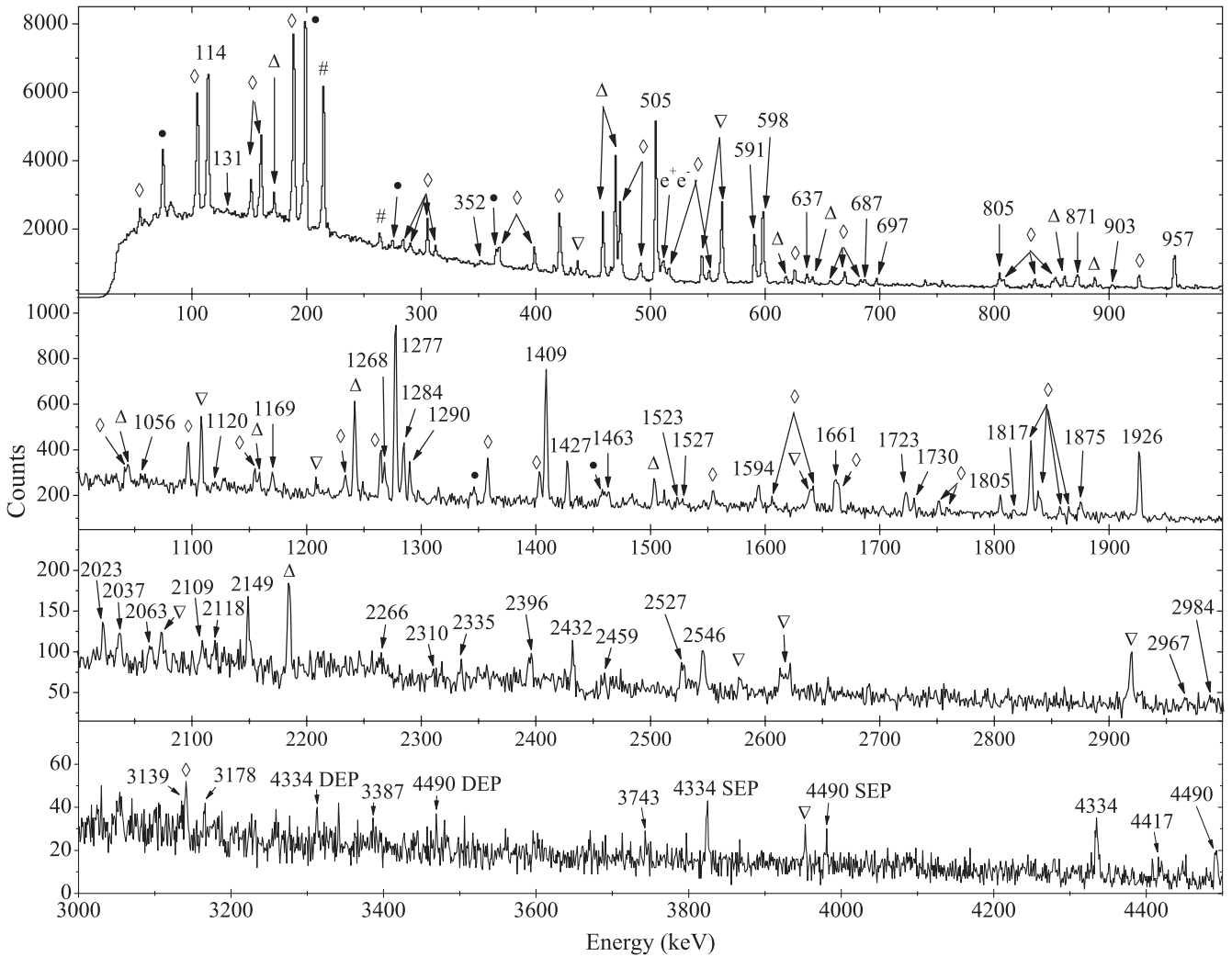


FIG. 1. Saturation spectrum in coincidence with the  $\beta$  detectors obtained in the LeRIBSS data run with a purified  $^{77}\text{Cu}$  beam. The  $\gamma$ -ray peaks assigned to  $^{77}\text{Cu}$  are indicated by their energy in keV, with single and double escape peaks labeled SEP and DEP, respectively. Other members of the two decay chains are indicated as follows:  $^{77}\text{Zn}$  ( $\diamond$ ),  $^{76}\text{Zn}$  ( $\bullet$ ),  $^{77}\text{Ga}$  ( $\triangle$ ),  $^{76}\text{Ga}$  ( $\nabla$ ), and  $^{77}\text{Ge}$  ( $\#$ ).

$\gamma$  rays from high-lying states where mainly direct feeding will occur have a very precise  $Q_{\text{eff}}$  but an imprecise  $\beta_{\text{eff}}$  owing to low statistics. For  $Q_{\text{eff}} \leq 5$  MeV, averages for several states fed in the decays of  $^{76,77}\text{Zn}$  and  $^{76}\text{Ga}$  with similar  $Q_{\text{eff}}$  values were used. Above this energy,  $\gamma$  rays from the decay of  $^{77}\text{Cu}$  were used as reported in Table I. For each level, it was assumed that some percentage of the unobserved feeding, as indicated in the table, could come from feeding to states in a 0.5-MeV window just below the neutron separation energy. For states where no missed feeding is assumed, a nominal uncertainty of 50 keV was used. For states with missed feeding assumed, the value of  $Q_{\text{eff}}$  is reduced and the uncertainty becomes much larger. Data points used in estimating  $\beta_{\text{eff}}$  are plotted in Fig. 4. The data were fit to a linear function where the weighting factor included the uncertainties in both  $\beta_{\text{eff}}$  and  $Q_{\text{eff}}$ . Table II reports information on  $\beta_{\text{eff}}$  for other levels and compares the value of  $Q_{\text{eff}}$  obtained from our decay scheme (Fig. 3) to the value estimated from the  $\beta_{\text{eff}}$  curve (Fig. 4). Relative intensities for all  $\gamma$  rays associated with  $^{77}\text{Cu}$  decay were

scaled using  $\beta_{\text{eff}}$  values from direct measurement of strong transitions or estimates based on the observed decay scheme with the assumption that 50% of any unobserved feeding to a level comes from the states near the neutron separation energy. For the latter group of  $\gamma$  rays, the adjustment for  $\beta_{\text{eff}}$  usually was within the statistical uncertainty so that the compensation for  $\beta_{\text{eff}}$  primarily resulted in an increased uncertainty in the relative intensity. It is evident in this analysis that, except for the levels at 1363 and 2235 keV, which have the highest values of  $\beta_{\text{eff}}$ , the observed feedings are overestimates.

### III. RESULTS AND DISCUSSION

The only published information on states in  $^{77}\text{Zn}$  prior to these experiments was a 1.05-s  $E3$  isomer at 772 keV and states at 114 and 803 keV observed in the  $\beta n$  branch of  $^{78}\text{Cu}$  decay [13,14]. We were able to identify 72  $\gamma$  rays associated with the  $\beta$  decay of  $^{77}\text{Cu}$  and produce the decay scheme

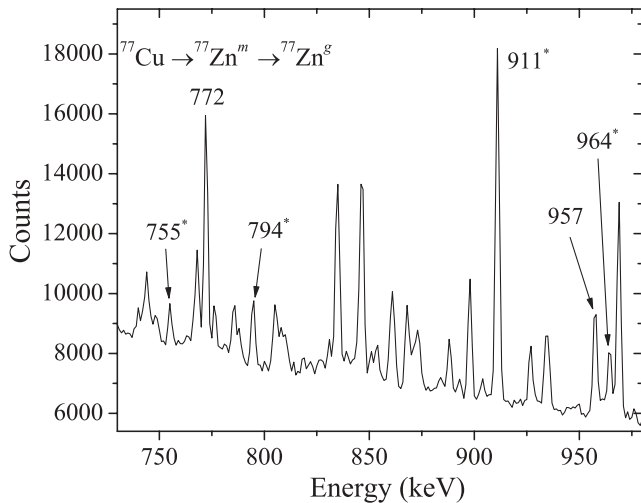


FIG. 2. Portion of the  $\gamma$ -ray singles saturation spectrum from the LeRIBSS data run showing the presence of the 772-keV  $\gamma$  ray from de-excitation of  $^{77}\text{Zn}^m$ . Also labeled are lines from the  $\beta$  decay of  $^{228}\text{Ac}$ (\*) in the background and the 957-keV line from  $^{77}\text{Cu}$   $\beta$  decay.

shown in Fig. 3, where the intensities shown are normalized relative to the 505-keV  $\gamma$  ray. The intensities for stronger transitions that could be fit cleanly were taken from the  $\gamma$ -ray singles spectrum, whereas the intensities for other transitions were taken from a  $\beta$ -gated spectrum and were corrected for the observed variation in  $\beta$  detection efficiency. Summing corrections based on the proposed decay scheme were also included. All  $\gamma$  rays associated with this decay were observed to have the correct time behavior in the MTC cycle as well as  $\gamma$ - $\gamma$  coincidence relationships with the stronger transitions. All  $\gamma$  rays observed in the spectrum with a relative intensity of 2% or greater were placed in the level scheme or firmly assigned to the decay of a daughter activity. Some weaker  $\gamma$  rays, with relative intensities between 1% and 2%, have the proper time behavior to be associated with  $^{77}\text{Cu}$  decay

TABLE I. Information on  $\beta_{\text{eff}}$  for  $\gamma$  rays associated with  $^{77}\text{Cu}$  decay used in determining the  $\beta$  efficiency curve.

Level energy (keV)	$\gamma$ -ray energy (keV)	$\beta_{\text{eff}}$ (%)	$Q_{\text{eff}}^{\text{a}}$ (MeV)	Feeding <sup>b</sup> (%)	$Q_{\text{eff}}^{\text{c}}$ (MeV)
4605	4490	46(8)	5.54(1)	0	5.54(5)
4334	4334	51(7)	5.81(1)	0	5.81(5)
3386	2023	49(3)	6.40(1)	100	5.87(32)
	2109				
3823	2546	50(6)	6.32(1)	25	6.20(22)
1277	505	57.3(6)	6.92(10)	100	6.67(11)
	1277				
3204	1926	60(3)	6.94(1)	0	6.94(5)
2235	957	65.3(18)	7.67(10)	0	7.67(10)
1363	591	66.2(19)	7.75(9)	0	7.75(9)

<sup>a</sup>Based on feedings in the decay scheme shown in Fig. 3.

<sup>b</sup>Percentage of unobserved feeding assumed to come from higher-lying states.

<sup>c</sup>Adjusted for possible feeding from unobserved  $\gamma$  rays.

TABLE II. Information on  $\beta_{\text{eff}}$  for additional  $\gamma$  rays associated with  $^{77}\text{Cu}$  decay that show a significant deviation from the curve in Fig. 4.  $\gamma$  rays are listed according to their level of origin.

Level energy (keV)	$\gamma$ -ray energy (keV)	$\beta_{\text{eff}}$ (%)	$Q_{\text{eff}}^{\text{a}}$ (MeV)	$Q_{\text{eff}}^{\text{b}}$ (MeV)
114	114	53.0(14)	7.25(18)	6.28(14)
801	687	55(9)	9.34(1)	6.5(10)
1284	1284	55(4)	8.46(12)	6.5(4)
1408	1408	51.3(18)	7.74(16)	6.11(18)
1427	1427	56(4)	8.05(15)	6.6(4)
1875	467	54(6) <sup>c</sup>	7.67(24)	6.3(6)
	1875			
2082	805	42.3(20)	6.0(5)	5.20(20)
2654	1290	41(4)	7.49(1)	5.1(4)
3083	1805	53(6)	7.06(1)	6.2(6)

<sup>a</sup>Based on feedings in the decay scheme shown in Fig. 3.

<sup>b</sup>Estimated from the  $\beta$  efficiency curve (Fig. 4).

<sup>c</sup>Average of values for 467- and 1875-keV  $\gamma$  rays.

but could not be placed in the decay scheme due to a lack of solid  $\gamma$ - $\gamma$  coincidence information (Table III). It is possible that some of these transitions could directly feed the ground or isomeric states. All transitions and excited states in the decay scheme are supported by  $\gamma$ - $\gamma$  coincidences, although there is some uncertainty in the placement leading to the “dashed” levels and transitions. Bound excited states are observed up to the neutron separation energy at  $S_n = 4.557(5)$  MeV [15]. One state, at 4.605 MeV, was found to lie about 50 keV above the  $S_n$  value.

One unique feature of the decay scheme presented in Fig. 3 is that, except for the 1277-keV level, no states have strong transitions to both the isomeric state and the ground/first excited state. In fact, only six states have transitions to either of the two lowest energy states and the 1277-keV level. None of the strongest  $\gamma$  rays are in coincidence with the 114-keV ground-state transition (Fig. 5) and the 114-keV  $\gamma$  ray sees primarily higher energy lines. In the RO experiment, where the weaker transitions were not observed, this arrangement suggested the possibility of a  $\beta$ -decaying isomer in  $^{77}\text{Cu}$ . In the LeRIBSS experiment we concentrated on looking into this possibility. A comparison of the half-lives for the 114-keV and 505- + 1277-keV  $\gamma$  rays (Fig. 6) shows excellent agreement, suggesting a single  $\beta$ -decaying state for  $^{77}\text{Cu}$  with a half-life of

TABLE III. Unplaced  $\gamma$  rays associated with  $^{77}\text{Cu}$  decay.

Energy (keV)	$I_{\gamma(\text{rel})}^{\text{a}}$ (%)	$I_{\gamma(\text{abs})}^{\text{b}}$ (%)
1795.0(6)	1.0(4)	0.19(8)
2063.0(6)	1.8(7)	0.34(13)
2085.7(4)	1.6(4)	0.31(8)
2310.5(6)	1.1(4)	0.21(8)
2989.3(5)	1.6(4)	0.31(8)
3133.2(5)	1.6(4)	0.31(8)

<sup>a</sup>Relative to the 505-keV  $\gamma$  ray.

<sup>b</sup>Per  $^{77}\text{Cu}$  decay.

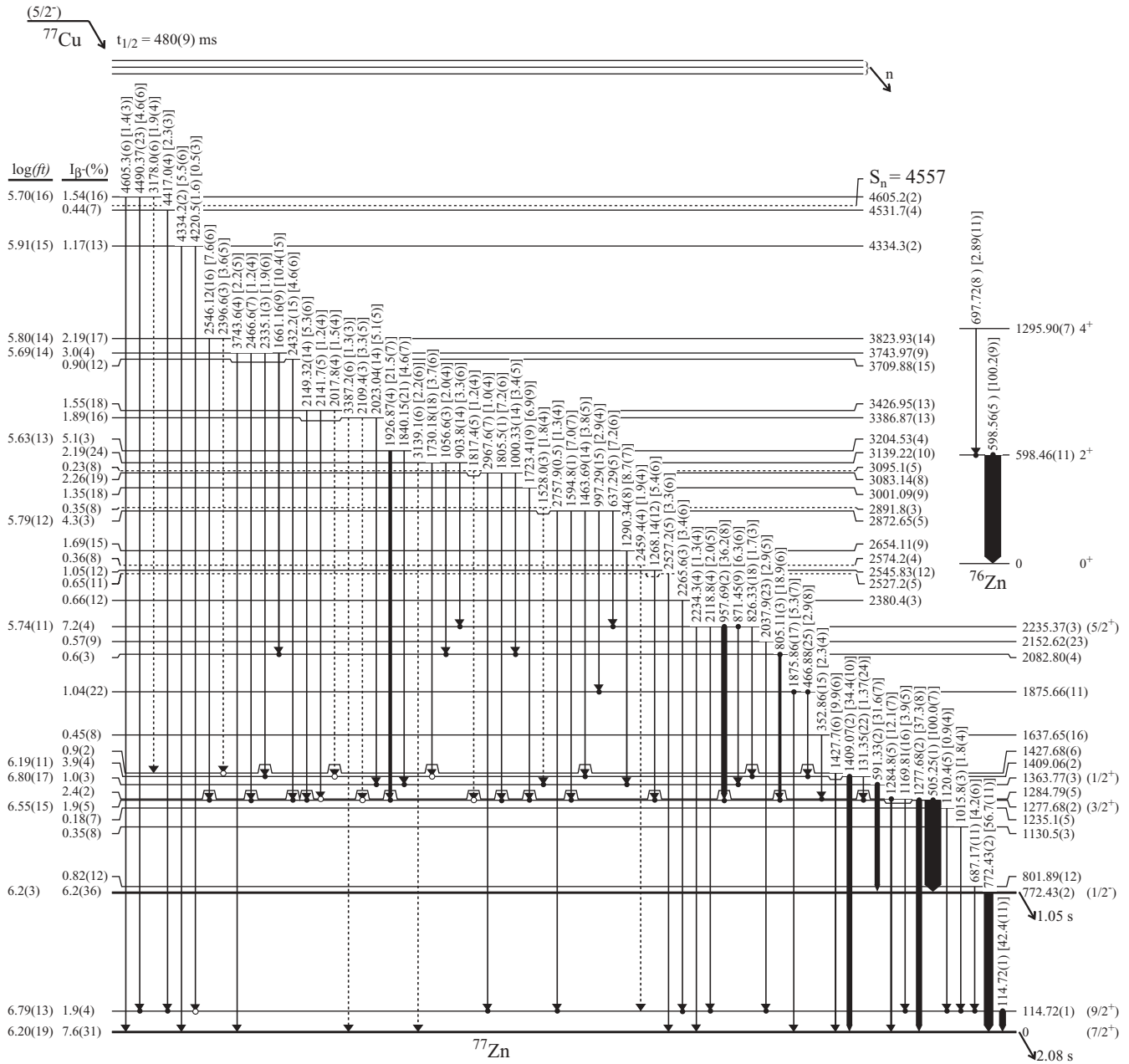


FIG. 3. Proposed scheme for  $^{77}\text{Cu}$  decay to excited states in  $^{76,77}\text{Zn}$ . Relative intensities of  $\gamma$  rays to the 505-keV transition are indicated in brackets. Filled circles indicate  $\gamma$ - $\gamma$  coincidences seen both ways, whereas open circles indicate coincidences observed only from the upper transition. Transitions and levels without strong coincidence relationships and/or other linking transitions are indicated by dashed lines. Level feedings are based on the measured absolute branching ratio for the 505-keV transition [19.1(6)%] as described in the text. All energies are in keV.

480(9) ms. However, in principle, these results cannot exclude a  $^{77}\text{Cu}$  isomer with a half-life close to that of the ground state and nearly the same  $\beta n$  emission probability.

The strongest transition observed in the decay of  $^{77}\text{Cu}$  to states in  $^{77}\text{Zn}$  is at 505 keV. The absolute intensity of this  $\gamma$  ray was determined in the RO experiment by comparing the peak area in a  $\gamma$ -ray singles spectrum to the number of  $^{77}\text{Cu}$  ions identified and counted in the IC, with corrections made for absolute efficiency and coincidence summing. Values were obtained from measurements with an MTC cycle and

in saturation, yielding an average value of  $19.1\% \pm 0.6\%$  (see Fig. 7). A similar technique was used to establish the absolute branching ratios for the 772-keV  $\gamma$  ray from the internal transition (IT) decay of  $^{77}\text{Zn}^m$  and the 189-, 199-, and 563-keV  $\gamma$  rays from the  $\beta$  decays of  $^{77}\text{Zn}^g$ ,  $^{76}\text{Zn}$ , and  $^{76}\text{Ga}$ , respectively, as described in the following paragraphs (see Fig. 7). For the latter cases, the LeRIBSS data were also used, with the absolute normalization made relative to the 505-keV  $\gamma$  ray. This absolute normalization was also used to determine the apparent absolute feedings to the levels shown in Fig. 3. It

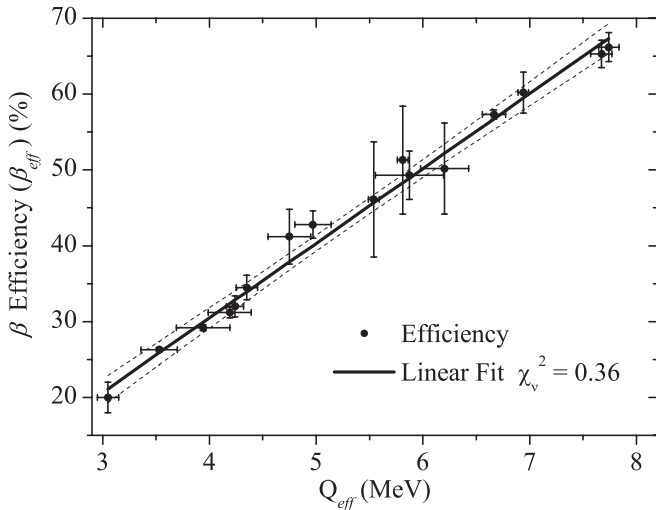


FIG. 4. The  $\beta$  detection efficiency ( $\beta_{\text{eff}}$ ) as a function of the effective  $Q$  value ( $Q_{\text{eff}}$ ) for the LeRIBSS measurement. The solid line is from a fit to the data, whereas the dashed lines show the  $\pm 2\sigma$  limits.

is obvious that the decay of  $^{77}\text{Cu}$  is highly fragmented, weakly feeding a large number of states. Because some  $\gamma$  rays from this decay could have intensities below our detection limit, these feedings should only be considered as the apparent feedings to the levels (upper limits). Corresponding lower limits for

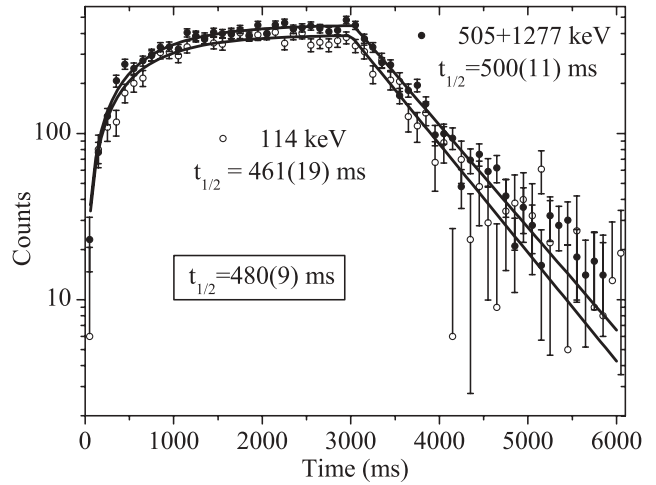


FIG. 6. Half-life curves for  $\gamma$  rays depopulating the 114- and 1277-keV levels. Data were fit in both the growth and the decay portions of the curve, to optimize statistics, using a nonlinear least-squares fit routine. Data between 1 and 3 s have little effect on the fitted values, therefore the initial grow-in and decay portions determine the half-life.

the  $\log(ft)$  values for selected levels were determined using our half-life of 480(9) ms and a  $Q_\beta$  of 10.21(40) MeV for  $^{77}\text{Cu}$  [15,16]; they are shown in Fig. 3. Additional information

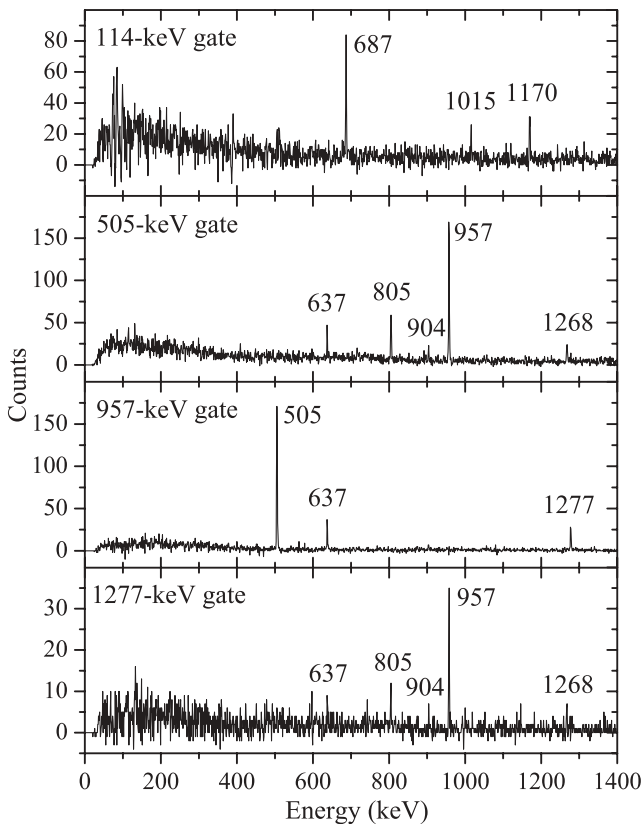


FIG. 5.  $\beta$ -gated  $\gamma$ -ray coincidence spectra for gates on the 114-, 505-, 957-, and 1277-keV transitions.

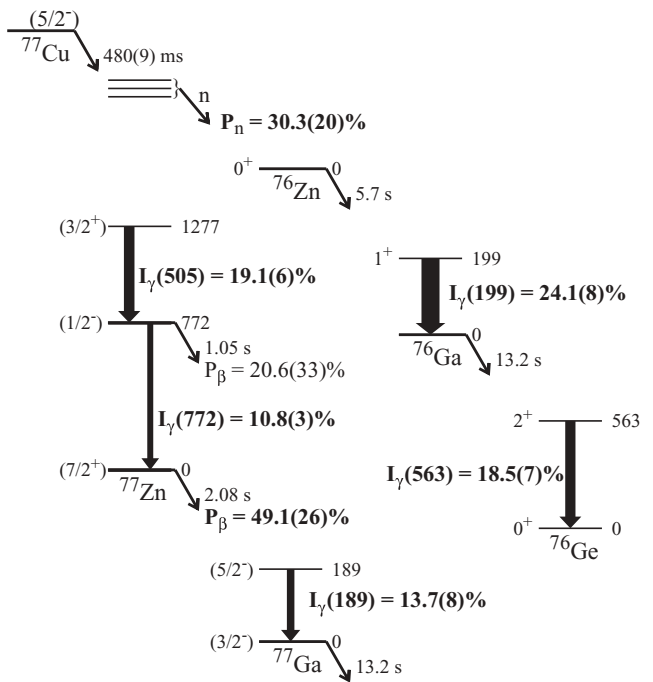


FIG. 7. Subset of the decay schemes of  $^{77}\text{Cu}$  and its daughter activities showing, in boldface, the directly measured absolute branching ratios per  $^{77}\text{Cu}$  decay. Intensities of the five  $\gamma$  rays were determined solely in the current experiments, whereas  $P_n$  and  $P_\beta$  for  $^{77}\text{Zn}^m$  incorporate additional information as discussed in the text. Also shown is the  $\beta$ -decay probability for  $^{77}\text{Zn}^m$  as derived from the other values. Energies shown (keV) are not to scale, whereas widths of the  $\gamma$ -ray transitions are.

on the decay scheme will be presented following a discussion of the measured absolute branching ratios.

Determination of the intensity for the 772-keV  $\gamma$  ray first required determination of the contamination to the peak area due to an unresolved background component from  $^{228}\text{Ac}$  belonging to the  $^{232}\text{Th}$  decay chain (see Fig. 2). The 772-keV line from the background has a relative intensity only 5.8% that of the 911-keV  $\gamma$  ray and should be comparable to the intensity of the 755-keV  $\gamma$  ray. It is evident in the spectrum that there is a significant component due to  $^{77}\text{Zn}^m$  IT decay. Because the detection efficiency for the background  $\gamma$  rays is different from that for the activity, a number of stronger  $\gamma$  rays from the decay of  $^{228}\text{Ac}$  were used to map out this variation and to extract the background component of the 772-keV peak area. The average value obtained for all measurements from the two experiments for the absolute branching ratio of the 772-keV  $\gamma$  ray per  $^{77}\text{Cu}$  decay is 10.8(3)% (see Fig. 7).

As suggested in Ref. [6],  $\beta$  decay from the  $^{77}\text{Zn}^m$   $1/2^-$  state will go preferentially by an allowed transition to the  $3/2^-$  ground state, or the  $1/2^-$  105-keV and  $3/2^-$  160-keV levels, of  $^{77}\text{Ga}$ , bypassing the  $5/2^-$  189-keV level, which would require a second forbidden decay. Therefore, the absolute branching ratio for the 189-keV  $\gamma$  ray should reflect the absolute branch from the decay of  $^{77}\text{Cu}$  that eventually feeds through the ground state, that is, the total intensity from the decay that ends up in the ground state by either direct population or  $\gamma$ -ray cascades. Comparison of the peak area to the number of  $^{77}\text{Cu}$  ions measured in the IC (RO experiment) or of the relative intensity to the 505-keV  $\gamma$  ray (LeRIBSS experiment) yields an absolute intensity of 13.7(8)% per  $^{77}\text{Cu}$  decay for the 189-keV  $\gamma$  ray. Combining this result with the published absolute branching ratio and internal conversion coefficient for the 189-keV  $\gamma$  ray from  $^{77}\text{Zn}^s$   $\beta$  decay [28.1(13)% and 0.013(2), respectively] [17] yields an average absolute branch of  $P_\beta = 49.1(26)\%$  per  $^{77}\text{Cu}$  decay (see Fig. 7).

In Ref. [6], we presented a  $\beta$ -delayed neutron emission probability of 30.0(27)% based on the measured absolute branching ratios of the 199- and 563-keV  $\gamma$  rays from the decays of  $^{76}\text{Zn}$  and  $^{76}\text{Ga}$ , respectively. This measurement used the peak areas of these  $\gamma$  rays, the number of  $^{77}\text{Cu}$  ions measured in the IC, and the published absolute branching ratios of the parent decays [ $I_\gamma(199\text{ keV}) = 77.5(18)\%$  and  $I_\gamma(563\text{ keV}) = 66(3)\%$ ] [17] as well as the internal conversion coefficient for the 199-keV  $\gamma$  ray [0.010(2)] [17]. A determination of this branch was also made for the LeRIBSS data using the intensities of these  $\gamma$  rays relative to that of the 505-keV  $\gamma$  ray. In both experiments, we observed that the value obtained from  $^{76}\text{Ga}$  decay was slightly lower than the value obtained from  $^{76}\text{Zn}$  decay. This is probably due to slight inaccuracies in the published absolute branching ratios and/or incomplete decay schemes. The average values for these decays from the two experiments are 31.6(12)% and 28.0(16)% for  $^{76}\text{Zn}$  and  $^{76}\text{Ga}$ , respectively, which are averaged to give our proposed value of 30.3(20)% (see Fig. 7).

Using the measured absolute branching ratios, it is now possible to estimate the direct feeding to the ground and isomeric states. Because we have measured the feeding from  $^{77}\text{Cu}$  decay through the  $\beta$ -delayed neutron branch and  $^{77}\text{Zn}^s$   $\beta$

decay, we can determine the absolute branch through  $\beta$  decay of  $^{77}\text{Zn}^m$  to be 20.6(33)%. Because the feeding by the IT decay from  $^{77}\text{Zn}^m$  is 10.8(3)% (see Fig. 7), the total feeding from  $^{77}\text{Cu}$  decay going through the isomeric state is 31.4(33)%, with 34(7)% of the decay out of this state going by IT decay. The isomeric state is observed to be fed only by the 505- and 591-keV  $\gamma$  rays, which have a combined absolute intensity of 25.2(8)%. Therefore, a total of 6.3(34)% of the feeding to this state has not been observed in  $\gamma$ -ray intensity. To determine the observed feeding to the ground state from prompt  $\gamma$  rays, it was first necessary to estimate the internal conversion coefficient for the 114-keV  $\gamma$  ray. In  $^{73,75}\text{Ge}$  the de-excitation  $\gamma$  ray between the lowest  $7/2^+$  and the lowest  $9/2^+$  states, with energies of about 65 keV, had measured internal conversion coefficients consistent with an almost-pure  $M1$  transition ( $\delta \approx 0.1$ ) [17]. Because the levels connected by the 114-keV  $\gamma$  ray are of the same spin and parity, and the energies are similar, we assume the same level of mixing for  $^{77}\text{Zn}$ ; this yields the internal conversion coefficient of 0.046(2), which was used to obtain a total relative intensity for the 114-keV  $\gamma$  ray of 42.4(11)%. We then observe a total absolute feeding from prompt  $\gamma$  rays and the IT transition of 41.1(11)%, whereas the intensity leaving this state is 49.1(26)%. The difference of 8.0(28)% corresponds to the unobserved intensity feeding this level. If the 114-keV  $\gamma$  ray is assumed to be a pure  $E2$  transition [ $\alpha = 0.394(11)$ ], then the unobserved feeding is only reduced to 5.3(29)%. For both the ground and the isomeric states, the missing intensity could come from unobserved prompt  $\gamma$  rays or from direct feeding in the  $\beta$  decay of  $^{77}\text{Cu}$ . The former case is a strong possibility, as the lower limit for assigning  $\gamma$  rays was a relative intensity of about 1% (0.2% absolute), but this seems to be a more likely possibility for the isomeric state than for the ground state. Finally, we note that the total observed intensity from prompt  $\gamma$  rays feeding either the ground or the isomeric state and the measured  $\beta$ -delayed neutron branch corresponds to a total of 96.5(24)% of the total decay intensity. Hence, there is only a small amount of unobserved feeding not accounted for in the current analysis.

The  $\beta$  decay of  $^{77}\text{Cu}$  is observed to feed the  $2_1^+$  and  $4_1^+$  states in even-even  $^{76}\text{Zn}$  [14,18] through the  $\beta$ -delayed neutron branch. The 598-keV  $\gamma$  ray has an intensity [100.2(9)%] equivalent to that of the 505-keV  $\gamma$  ray in the  $\beta$  branch. This equivalent intensity is not obvious in the  $\beta$ -gated spectrum shown in Fig. 1, as the  $\beta$  detection efficiency is much lower for the high-lying unbound states in  $^{77}\text{Zn}$  that are fed by this branch. Indeed, the measured  $\beta$  detection efficiency for the 598-keV  $\gamma$  ray (see Table II) is consistent with an average feeding in the  $\beta$  decay of  $^{77}\text{Cu}$  ( $Q_\beta = 10.21$  MeV) to states with an excitation energy of about 6.5 MeV in  $^{77}\text{Zn}$ . The 698-keV  $4_1^+ \rightarrow 2_1^+$  transition in  $^{76}\text{Zn}$ , with a relative intensity of 2.89(11)%, has a  $\beta$  detection efficiency (see Table II) consistent with average feeding to levels above 8 MeV in excitation. For both  $\gamma$  rays the intensity is taken from the  $\gamma$ -ray singles spectrum. Although the  $\beta$ -delayed neutron feeding to excited states is strong, 35(8)% of this decay branch appears to go to  $^{76}\text{Zn}^s$ .

The ground state of  $^{77}\text{Zn}$  has been proposed to be composed primarily of a  $(\nu g_{9/2})^3$  three-quasiparticle configuration [13].

The first excited state at 114 keV was first observed in the  $\beta$ -delayed neutron branch of  $^{78}\text{Cu}$  decay [14]. We observed a strong 114-keV  $\gamma$  ray that is coincident with numerous high-energy  $\gamma$  rays and is assigned as de-exciting the 114-keV level. This level has been assigned to have a large component of the  $J^\pi = 9/2^+$ ,  $\nu g_{9/2}$  single-particle configuration, similar to other Zn and Ge isotopes in this region [19,20]. The presence of the  $1/2^-$  isomeric state excludes any other option for this assignment, as a spin less than  $7/2$  or negative parity would provide an alternative path for the decay of the isomeric state. In addition, this assignment is supported by the lack of a coincidence between the 957-keV  $\gamma$  ray, the third-strongest transition observed in the decay, and the 114-keV  $\gamma$  ray, indicating that there are no transitions linking the 1277- and the 114-keV states. Although there is an apparent absolute feeding to the 114-keV state of 1.9(4)%, the  $\beta$  detection efficiency can only be explained if this missing feeding comes through states above 4 MeV in excitation (see Table II). Therefore, it is very likely that there is no direct feeding to this state. This level is observed to be fed by 13  $\gamma$  rays, all with relative intensities of less than 5%. The feeding states are most likely to have positive parity and spins greater than  $5/2$ . It is interesting to note that, of these 13 states, only five also have transitions to the ground state. This may be an indication of inhibition of these decays owing to the ground state's change to a three-quasiparticle structure. The opposite seems to be true for the 1409-, 1427-, and 1875-keV levels, which decay to the ground state but not the first excited state. This may be an indication that these states, which probably also have  $J \geq 5/2$ , are of a three-quasiparticle nature with a significant  $(\nu g_{9/2})^3$  component. The  $\beta$  detection efficiency for the 1409-keV  $\gamma$  ray suggests that all the feeding to this state comes from higher-lying levels.

The 1277-keV level is established based on the observation that both the 505- and the 1277-keV transitions are in coincidence with the 957-keV  $\gamma$  ray and not with each other (Fig. 5). In addition, the difference in the energy of these two  $\gamma$  rays matches the known energy of the 772-keV isomeric level. This level forms the backbone for the remainder of the level scheme, as only two currently observed transitions feed the isomeric level, whereas a large number of  $\gamma$  rays feed through the 1277-keV level. Because the 1277-keV level links to both the ground state,  $7/2^+$ , and the isomeric state,  $1/2^-$ , the spin-parity for this level is limited to  $3/2^\pm$  or  $5/2^\pm$ . A  $5/2^+$  assignment is precluded by the lack of even a weak  $E2$  transition to the first excited  $9/2^+$  state, and an  $E2$  transition to the ground state will dominate a  $M2$  transition to the isomer. A  $5/2^-$  assignment can also be rejected, as an  $E1$  ground-state transition should be stronger. Finally, a  $3/2^-$  assignment is rejected because an  $M1$  transition to the isomeric state should dominate. Hence the only logical assignment requires assuming the 505- and 1277-keV  $\gamma$  rays to be  $E1$  and  $E2$  transitions, respectively, yielding a spin-parity of  $3/2^+$  for the 1277-keV level.

The 1363-keV level is the only state other than the 1277-keV level that is observed to feed, by the 591-keV  $\gamma$  ray, the isomeric state. The position of this level is established by transitions from the levels at 2235 and 3204 keV, which also connect to the 1277-keV level. Because this state does

not decay to the ground state, the spin-parity must be  $1/2^\pm$  or  $3/2^-$  and connect to the isomeric level by an  $E1$  or  $M1$  transition. There is no evidence in the data to suggest even a weak 86-keV transition from this state to the 1277-keV level. This suggests a strong  $E1$  transition to the isomeric state and  $J^\pi = 1/2^+$ .

The 2235-keV level is established by numerous transitions to lower-lying states that feed both the  $J^\pi = 7/2^+$  ground state and the  $J^\pi = 1/2^-$  isomeric state. This state is somewhat unique in that it has a transition to almost all the states below it except for those that decay only to the first excited state. It is observed to decay by its strongest transition to the  $(3/2^+)$  1277-keV level, with weaker transitions to the  $(7/2^+)$  ground state,  $(9/2^+)$  114-keV level,  $(1/2^+)$  1363-keV level, and  $(J \geq 5/2)$  1409-keV level. However, no transition is observed going to the  $1/2^-$  isomeric state. The observation of transitions to states ranging from  $1/2^+$  to  $9/2^+$  implies a  $J^\pi = 5/2^+$  assignment if the spin-parity assignments for the other states are correct.

Based on the observed  $\beta$ -decay feedings for  $^{77}\text{Cu}$  into states of  $^{77}\text{Zn}$ , it is possible to estimate the ground-state spin-parity assignment for  $^{77}\text{Cu}$ . The arguments here are based on the assumption that the ground state will be dominated by either a  $\pi p_{3/2}$  or a  $\pi f_{5/2}$  orbital. The  $\log(ft)$  values shown in Fig. 3 do not strongly indicate any state fed by an allowed Gamow-Teller transition. An exception might be the state at 4605 keV, above the  $S_n$  energy of 4.557 MeV, which is undoubtedly directly fed in the  $\beta$  decay. As argued previously, the decay pattern of states that decay to the first excited state suggests a minimum spin of  $5/2$ . The 4605-keV level has transitions to both the ground state and the first excited state, which suggests that the spin is probably higher. An allowed  $\beta$  transition from a  $5/2^-$   $^{77}\text{Cu}^g$  to a  $7/2^-$  state would be consistent with this observation, whereas a second forbidden decay from a  $3/2^-$  state would be precluded. It is not obvious that either the  $7/2^+$  ground state or the  $1/2^-$  isomeric state is directly fed in the decay, as some  $\gamma$ -ray intensity is missing. The apparent  $\log(ft)$  values for both states are consistent with strong first forbidden decays. This makes sense for the ground state if  $J^\pi = 5/2^-$  for  $^{77}\text{Cu}^g$ . Conversely, if  $J^\pi = 3/2^-$  were assigned to the  $^{77}\text{Cu}^g$ , then we would expect a transition with an allowed Gamow-Teller component to the  $1/2^-$  isomeric state with much stronger direct  $\beta$  feeding. For comparison, the  $\beta$  decay of the  $\pi p_{3/2}$  ground state of  $^{73}\text{Cu}$  to the  $\nu p_{1/2}$  ground state of  $^{73}\text{Zn}$  has a measured  $\log(ft)$  value of 5.4 [21]. Such a low  $\log(ft)$  value for the decay of  $^{77}\text{Cu}$  would require feeding of about 35% to the isomeric state, which we did not find. All this evidence combines to suggest strongly that the ground state of  $^{77}\text{Cu}$  is the  $\pi f_{5/2}$  single-particle state, in agreement with the recent laser spectroscopy results obtained by Flanagan *et al.* [22].

#### IV. CONCLUSION

Experiments were performed with isobarically purified 225-MeV and 200-keV beams of  $^{77}\text{Cu}$ , with a directly measured intensity for the 225-MeV postaccelerated radioactive beam, resulting in considerable expansion of our knowledge



of the levels in  $^{77}\text{Zn}$  populated in  $\beta$ - $\gamma$  decay. A total of 64  $\gamma$  rays were placed, establishing 34 excited states up to the neutron separation energy and one state above the  $S_n$  value. Purified  $^{77}\text{Cu}$  activity, with a half-life of 480(9) ms measured in the low-energy experiment, was collected in front of the detector system, allowing us to trace the decay path down to the granddaughter activities of  $^{77}\text{Ga}$  ( $\beta$  branch) and  $^{76}\text{Ga}$  ( $\beta n$  branch). Absolute branching ratios were measured in the high-beam energy experiment, resulting in determination of the  $^{77}\text{Zn}^g$  and  $^{77}\text{Zn}^m$  feeding and the  $^{77}\text{Zn}^m$  IT-decay/ $\beta$ -decay branching ratio. Spin and parity assignments consistent with the observed feeding and decay pattern have been proposed for a number of levels in  $^{77}\text{Zn}$ . Based on the feeding to these states from the decay of the  $^{77}\text{Cu}$  activity, we propose  $J^\pi = 5/2^-$  for the ground state of this decay, supporting the theoretical prediction that the  $\pi f_{5/2}$  orbital drops below the  $\pi p_{3/2}$  orbital for  $Z = 29$   $^{77}\text{Cu}^g$ .

*Note added in proof.* Following the submission of this article, Patronis *et al.* published an article on the  $\beta$  decay of  $^{77}\text{Cu}$  [23]. Our results are in basic agreement with those in

Ref. [23] but include significantly greater detail and measured absolute branching ratios.

#### ACKNOWLEDGMENTS

We wish to acknowledge the Holifield Radioactive Ion Beam Facility (HRIBF) and staff for their help and the excellent quality of the neutron-rich beams. In addition, the engineering staff at the HRIBF deserves our thanks for their help in constructing the Low-energy Radioactive Ion Beam Spectroscopy Station beam line. Oak Ridge National Laboratory is managed by UT-Battelle, LLC, for the US Department of Energy under Contract No. DE-AC05-00OR22725. Additionally, this work was supported by US Department of Energy Grant Nos. DE-FG02-96ER41006, DE-FG02-96ER40983, DE-AC05-06OR23100, DE-FG02-96ER40978, and DE-FG05-88ER40407; National Nuclear Security Administration Grant No. DEFC03-03NA00143; Polish Ministry of Science and Higher Education Grant No. N N202 1033 33; and the Foundation for Polish Science.

- 
- [1] J. P. Schiffer, S. J. Freeman, J. A. Caggiano, C. Deibel, A. Heinz, C.-L. Jiang, R. Lewis, A. Parikh, P. D. Parker, K. E. Rehm, S. Sinha, and J. S. Thomas, *Phys. Rev. Lett.* **92**, 162501 (2004).
- [2] L. Gaudefroy, O. Sorlin, D. Beaumel, Y. Blumenfeld, Z. Dombárdi, S. Fortier, S. Franchoo, M. Gélín, J. Gibelin, S. Grévy, F. Hammache, F. Ibrahim, K. W. Kemper, K.-L. Kratz, S. M. Lukyanov, C. Monrozeau, L. Nalpas, F. Nowacki, A. N. Ostrowski, T. Otsuka, Yu.-E. Penionzhkevich, J. Piekarewicz, E. C. Pollacco, P. Roussel-Chomaz, E. Rich, J. A. Scarpaci, M. G. St. Laurent, D. Sohler, M. Stanoiu, T. Suzuki, E. Tryggestad, and D. Verney, *Phys. Rev. Lett.* **97**, 092501 (2006).
- [3] S. Franchoo, M. Huysse, K. Kruglov, Y. Kudryavtsev, W. F. Mueller, R. Raabe, I. Reusen, P. Van Duppen, J. Van Roosbroeck, L. Vermeeren, A. Wöhr, H. Grawe, K.-L. Kratz, B. Pfeiffer, and W. B. Walters, *Phys. Rev. C* **64**, 054308 (2001).
- [4] T. Otsuka, T. Suzuki, R. Fujimoto, H. Grawe, and Y. Akaishi, *Phys. Rev. Lett.* **95**, 232502 (2005).
- [5] J. Dobaczewski, N. Michel, W. Nazarewicz, M. Ploszajczak, and J. Rotureau, *Prog. Part. Nucl. Phys.* **59**, 432 (2007).
- [6] J. A. Winger, S. V. Ilyushkin, K. P. Rykaczewski, C. J. Gross, J. C. Batchelder, C. Goodin, R. Grzywacz, J. H. Hamilton, A. Korgul, W. Królas, S. N. Liddick, C. Mazzocchi, S. Padgett, A. Piechaczek, M. M. Rajabali, D. Shapira, E. F. Zganjar, and I. N. Borzov, *Phys. Rev. Lett.* **102**, 142502 (2009).
- [7] C. J. Gross, K. P. Rykaczewski, D. Shapira, J. A. Winger, J. C. Batchelder, C. R. Bingham, R. K. Grzywacz, P. A. Hausladen, W. Królas, C. Mazzocchi, A. Piechaczek, and E. F. Zganjar, *Eur. Phys. J. A* **25**, S01, 115 (2005).
- [8] HRIBF's LeRIBSS web site, <http://www.phy.ornl.gov/hribf/equipment/leribss/>.
- [9] R. Grzywacz, *Nucl. Instrum. Methods Phys. Res. B* **204**, 649 (2003).
- [10] J. A. Winger, S. V. Ilyushkin, A. Korgul, C. J. Gross, K. P. Rykaczewski, J. C. Batchelder, C. Goodin, R. Grzywacz, J. H. Hamilton, W. Królas, S. N. Liddick, C. Mazzocchi, C. Nelson, S. Padgett, A. Piechaczek, M. M. Rajabali, D. Shapira, and E. F. Zganjar, in *Proceedings of the International Nuclear Physics Conference (INPC2007)*, Tokyo (2008), Vol. 2, p. 293.
- [11] J. A. Winger, S. V. Ilyushkin, A. Korgul, C. J. Gross, K. P. Rykaczewski, J. C. Batchelder, C. Goodin, R. Grzywacz, J. H. Hamilton, W. Królas, S. N. Liddick, C. Mazzocchi, C. Nelson, S. Padgett, A. Piechaczek, M. M. Rajabali, D. Shapira, and E. F. Zganjar, in *Proceedings of the XXXth Mazurian Lakes Conference on Physics, Piaski, Poland, September 2–9, 2007* [*Acta Phys. Pol. B* **39**, 525 (2008)].
- [12] S. V. Ilyushkin, J. A. Winger, A. Korgul, C. J. Gross, K. P. Rykaczewski, J. C. Batchelder, C. Goodin, R. Grzywacz, J. H. Hamilton, W. Królas, S. N. Liddick, C. Mazzocchi, S. Padgett, A. Piechaczek, M. M. Rajabali, D. Shapira, and E. F. Zganjar, in *Proceedings of the Fourth International Conference on Fission and Properties of Neutron-Rich Nuclei, Sanibel Island, FL, USA, November 11–17, 2007*, edited by J. H. Hamilton, A. V. Ramayya, and H. K. Carter (World Scientific, Singapore, 2008), p. 687.
- [13] B. Ekström, B. Fogelberg, P. Hoff, E. Lund, and A. Sangariyavanish, *Phys. Scr.* **34**, 614 (1986).
- [14] J. Van Roosbroeck, H. De Witte, M. Gorska, M. Huysse, K. Kruglov, D. Pauwels, J.-Ch. Thomas, K. Van de Vel, P. Van Duppen, S. Franchoo, J. Cederkall, V. N. Fedoseyev, H. Fynbo, U. Georg, O. Jonsson, U. Köster, L. Weissman, W. F. Mueller, V. I. Mishin, D. Fedorov, A. De Maesschalck, N. A. Smirnova, and K. Heyde, *Phys. Rev. C* **71**, 054307 (2005).
- [15] J. Hakala, S. Rahaman, V.-V. Elomaa, T. Eronen, U. Hager, A. Jokinen, A. Kankainen, I. D. Moore, H. Penttilä, S. Rintantila, J. Rissanen, A. Saastamoinen, T. Sonoda, C. Weber, and J. Äystö, *Phys. Rev. Lett.* **101**, 052502 (2008).
- [16] G. Audi, A. H. Wapstra, and C. Thibault, *Nucl. Phys.* **A729**, 337 (2003).
- [17] National Nuclear Data Center, ENSDF database, <http://www.nndc.bnl.gov>.
- [18] J. A. Winger, J. C. Hill, F. K. Wahn, E. K. Warburton, R. L. Gill, A. Piotrowski, R. B. Schuhmann, and D. S. Brenner, *Phys. Rev. C* **42**, 954 (1990).

- [19] D. von Ehrenstein and J. P. Schiffer, *Phys. Rev.* **164**, 1374 (1967).
- [20] W. A. Yoh, S. E. Darden, and S. Sen, *Nucl. Phys.* **A263**, 419 (1976).
- [21] M. Huhta, P. F. Mantica, D. W. Anthony, P. A. Lofy, J. I. Prisciandaro, R. M. Ronningen, M. Steiner, and W. B. Walters, *Phys. Rev. C* **58**, 3187 (1998).
- [22] K. T. Flanagan, P. Vingerhoets, M. Avgoulea, J. Billowes, M. L. Bissell, K. Blaum, B. Cheal, M. De Rydt, V. N. Fedosseev, D. H. Forest, Ch. Geppert, U. Köster, M. Kowalska, J. Krämer, K. L. Kratz, A. Krieger, E. Mané, B. A. Marsh, T. Materna, L. Mathieu, P. L. Molkanov, R. Neugart, G. Neyens, W. Nörtershäuser, M. D. Seliverstov, O. Serot, M. Schug, M. A. Sjoedin, J. R. Stone, N. J. Stone, H. H. Stroke, G. Tungate, D. T. Yordanov, and Yu. M. Volkov, *Phys. Rev. Lett.* **103**, 142501 (2009).
- [23] N. Patronis, H. De Witte, M. Gorska, M. Huyse, K. Kruglov, D. Pauwels, K. Van de Vel, P. Van Duppen, J. Van Roosbroeck, J.-C. Thomas, S. Franchoo, J. Cederkall, V. N. Fedoseyev, H. Fynbo, U. Georg, O. Jonsson, U. Köster, T. Materna, L. Mathieu, O. Serot, L. Weissman, W. F. Mueller, V. I. Mishin, and D. Fedorov, *Phys. Rev. C* **80**, 034307 (2009).